Co-current toroidal rotation driven and turbulent stresses with resonant magnetic perturbations in the edge plasmas of the J-TEXT tokamak

K. J. Zhao,[1] Y. J. Shi,[2] H. Liu, [2] P. H. Diamond,[3] F. M. Li,[2] J. Cheng,[1] Z. P. Chen,[2] L. Nie,[1] Y. H. Ding,[2] Y. F. Wu,[1] Z. Y. Chen,[2] B. Rao,[2] Z. F. Cheng,[2] L. Gao,[2] X. Q. Zhang,[2] Z. J. Yang,[2] N. C. Wang,[2] L. Wang,[2] W. Jin,[2] J. Q. Xu,[1] L. W. Yan,[1] J. Q. Dong,[1] G. Zhuang,[2] and J-TEXT team

1. Southwestern Institute of Physics, P. O. Box 432, Chengdu, China

2. College of Electrical and Electronic Engineering, Huazhong University of Science and Technology, Wuhan Hubei, 430074, China

3. Center for Momentum Transport and Flow Organization, University of California at San Diego, California 92093, USA

Abstract: The acceleration of the co-current toroidal rotations around resonant surfaces by resonant magnetic perturbations (RMPs) through turbulence is presented. These experiments were performed using a Langmuir probe array in the edge plasmas of the J-TEXT tokamak. This study aims at understanding the RMP effects on edge toroidal rotations and exploring its control method. With RMPs, the flat electron temperature T_e profile due to magnetic islands appears around resonant surfaces [*K. J. Zhao et al., Nucl Fusion, **55**, 073022 (2015)*]. When the resonant surface is closer to the last closed flux surface, the flat T_e profile vanishes with RMPs. In both cases, the toroidal rotations significantly increase in the direction of the plasma current around resonant surfaces with RMPs. The characteristics of turbulence are significantly affected by RMPs around resonant surfaces. Turbulence intensity profile changes and the poloidal wave vector k_θ increases with RMPs. The power fraction of the turbulence components in the ion diamagnetic drift direction increases with RMPs.

The measurements of turbulent Reynolds stresses are consistent with that the toroidal flows can be driven by turbulence. The estimations of the energy transfer between turbulence and toroidal flows suggest that turbulence energy transfers into toroidal flows. The result has the implication of the intrinsic rotation being driven by RMPs via turbulence.

1. Introduction

Interaction of magnetohydrodynamic (MHD) structures and flows is a subject of general interest in physics. Typical examples include magnetic braking of stellar rotation [1], angular momentum transport in astrophysical disks [2, 3], and dynamics of the earth core and geodynamo [4]. In fusion plasmas, the study of interactions between plasma flows and resonant magnetic perturbations (RMPs) aims at understanding and controlling plasma confinement and transport. RMPs have significant effects on the profiles and cross field transport [5–14], and are applied to mitigate the large scale edge local mode (ELM) in tokamak plasmas [15].

The toroidal rotation has been widely recognized to play an important role in plasma confinement improvement [16-17] and MHD stabilization [18-19] in tokamaks and in helical devices. There are various driving mechanisms for toroidal rotations and some of them have already been well documented. They are: external momentum input, such as neutral beam injection; spontaneous/intrinsic rotation without apparently momentum input [20-25]. The intrinsic rotation can be caused by residual Reynolds stresses due to turbulence. The residual stress is a part of the total Reynolds stress. It is independence of the velocity and velocity gradient, and only depends on the characteristics of turbulence, the temperature gradient, density gradient and pressure gradient etc. A new turbulent acceleration term which has different physics from the residual stress was found to drive the co-current rotation using gyrokinetic theory [26]

RMPs can generate not only stochastic magnetic fields, but also coherent magnetic islands. RMP-induced stochastic regions and magnetic islands have strong effects on turbulence [9-14, 27]. The common feature is that the radial electric field E_r increases

in stochastic and magnetic island regions [11-13, 27-29]. The phase delay between the plasma edge density and electron temperature depends on the relative rotation of the RMP field and the toroidal plasma rotation [30]. The plasma flow is also influenced by RMPs [11, 31]. The RMP braking effects on the toroidal rotation were observed in the core plasmas in most devices [32]. The opposite effects - the acceleration of toroidal rotations due to RMPs - were detected in a few devices. With small injected neutral beam momentum, the toroidal rotation is accelerated in a direction counter to the plasma current due to RMPs [33]. The deeply penetrating RMPs of m/n=3/1 mode configuration increases the toroidal plasma rotation and the toroidal rotation is always in the direction of the plasma current [34]. In the edge tokamak plasmas, the acceleration of the toroidal rotation due to RMPs was also measured [27-29]. However, the correlation between the acceleration of toroidal rotations and turbulence with RMPs has not been studied although this is a crucial issue because of its relevance to intrinsic rotation.

Here, the acceleration of the toroidal rotation in the direction of the plasma current around resonant surface in the edge tokamak plasmas with RMPs is presented. The characteristics of turbulence around resonant surface are varied when the RMP coils are applied. With RMPs, the turbulence energy around resonant surface transfers into toroidal flows. This observation suggests that the acceleration of the toroidal flow is relevant to the change of the turbulent characteristics around resonant surface with RMPs.

The rest of this work is organized as follows. The experimental set-up is given in section 2. The experimental results, described in section 3, include the acceleration of the toroidal rotation with RMPs, the radial dependences of the plasma parameters with RMPs, RMP effects on turbulence characteristics and turbulent Reynolds stress, etc. Section 4 presents the conclusion and discussion.

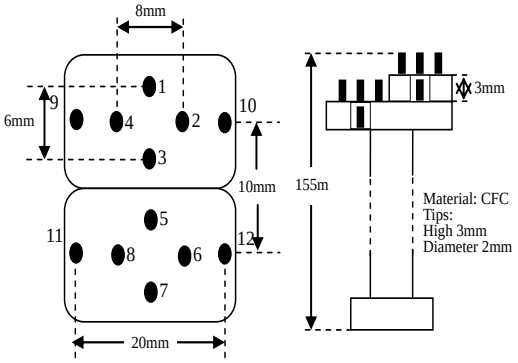

Figure 1 (color online) Configuration of a fast reciprocating probe array.

2. Experiment setup

The experiments presented here were conducted in Ohmic plasmas with circular cross section on the J-TEXT tokamak. The major and minor radii of the J-TEXT tokamak are R = 1.05 m and a = 0.255 m, respectively [35]. The plasma parameters for the experiments are the toroidal magnetic field B_t = 1.5-2.0 T, the plasma current I_p = 150-180 kA, the line averaged electron density N_e = 1-3X$10^{19} m^{-3}$, and the edge safety factor q_a = 3.1-4.3. A set of coils, called a dynamic RMP, has been installed inside the vessel on J-TEXT to study the interaction between helical perturbations and magnetized plasmas, and explore a possible method for control of tearing modes [36]. In the present study, the static configuration of RMP was used. The base mode and strength of the magnetic perturbation were varied by adjusting the power supply to the coils. The perturbation field strength of B_r ~5.42 X10^{-5} T for m/n = 3/1 mode, and of ~1.16 X10^{-5} T for m/n = 4/1 mode can be obtained for 1kA in the coils assuming no plasma response. Here, m and n are the poloidal and toroidal mode numbers, respectively. The maximum RMP current is 6.5 kA. A fast reciprocating probe array with two steps and 12 tips as shown in figure 1 yields the profiles of floating potential, temperature, density, Mach number, etc.. It was mounted on the top of the tokamak. The length and diameter of the tips are 3 mm and 2 mm, respectively. The digitizer can handle fluctuation data up to 2 MHz.

3. Experimental results

3.1 Increase of edge toroidal rotation velocity near resonant surface with RMPs

The increase of the edge toroidal rotation velocity is detected with resonant magnetic perturbations in the edge plasmas of the J-TEXT tokamak. Figure 2 provides the radial profiles of the edge toroidal rotation velocity with RMP current scan. The positive (negative) sign of the toroidal velocity means in the co-current direction (counter-current direction). The edge safety factor and the line averaged electron density are q_a = 3.1 and N_e = 2.2x$10^{19} m^{-3}$, respectively. The toroidal rotation is measured with a Mach probe array. The Mach number can be estimated as

M_{mach}=0.4ln($I_{s\text{-}up}$/ $I_{s\text{-}down}$) , where $I_{s\text{-}up}$ and $I_{s\text{-}down}$ are the sheath currents collected on two Mach probe tips at the up- and down-stream sides, respectively. The toroidal velocity can be calculated as $V_\varphi \approx M_{mach} C_s$. The C_s is ion sound speed as $\sim \sqrt{2T_e / m_i}$, here T_e and m_i are the electron temperature and the ion mass, respectively. Inside the LCFS, the toroidal rotation velocity slightly increases first in the co-current direction as the RMP current increases. When the RMP current is above a threshold value ~5kA, the toroidal velocity around the q=3 resonant surface in the interval -1.0< Δr < -0.2cm rapidly increases in the co-current direction, by up to 10km/s. Here, Δr means the distance from the measurement position to the LCFS and minus means inside the LCFS. In the scrape-off layer (SOL), the toroidal rotation near Δr = 0.8cm also increases first in the co-current direction for increasing RMP current,

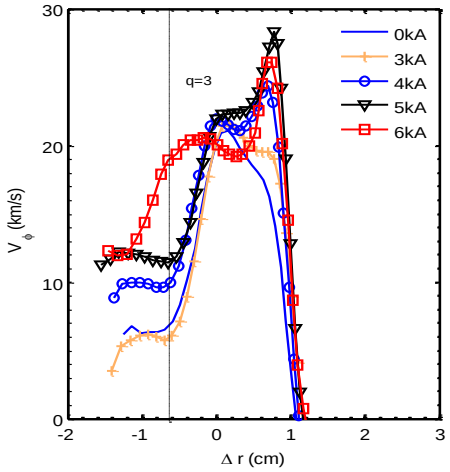

Figure 2 (color online) The radial profiles of toroidal rotation velocity with RMP current scan. [The vertical dashed-dot line indicated the q=3 resonant surface, B_t~1.6T, I_p~165kA, q_a=3.1, N_e~2.2x10^{19}m^{-3}].

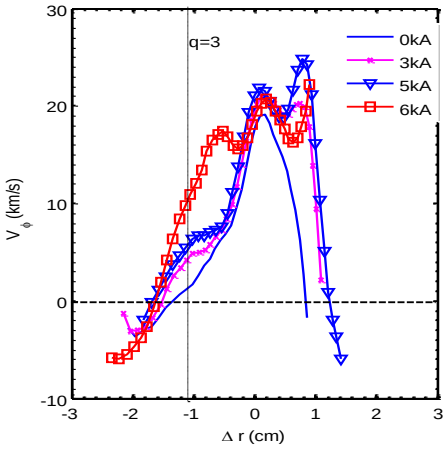

Figure 3 (color online) The radial profiles of toroidal rotation velocity with RMP current scan. [The vertical dashed-dot line indicated the q=3 resonant surface, B_t~1.6T, I_p~160kA, q_a=3.2, N_e~3.0x10^{19}m^{-3}].

but when the RMP current is ~6kA, the toroidal velocity starts to drop. Compared with the cases inside the LCFS and in the SOL region, the effects of RMPs on the toroidal rotation at the LCFS of Δr ~ 0.0cm are much different. With RMPs, the toroidal rotation changes little at the LCFS. The evolutions of the toroidal rotations in the SOL region might come from the mixing effects of the secondary limiter at Δr

~1cm due to the RMP assembly and the RMPs. We will not discuss it more. In this paper, the RMP effects on the toroidal rotation around resonant surface will be focused on.

The RMP effects on the edge toroidal rotations in the resonant layers were examined further with edge safety factor q_a=3.2 and the line averaged density N_e~3.0x10^{19}m^{-3}. Figure 3 shows the radial profiles of the toroidal rotation velocity with RMP current scan. The evolutions of the toroidal rotation around the resonant surface with RMP current are similar to the cases with q_a = 3.1, i.e., when RMP current is above ~5kA, the toroidal rotation rapidly increases in the q=3 resonant layer.

3.2 Radial dependences of plasma parameters with 3/1 RMPs

The radial dependences of plasma parameters with and without 3/1 RMPs at q_a=3.2 are studied. Figures 4 (a)-(d) show the radial profiles of the toroidal rotation velocities, the electron temperatures, the electron densities, and the radial electric fields (E_r), respectively. The RMP current is 6kA and produces a relative magnetic perturbation B_r/B_0 ~ 2 X 10^{-4} for the m/n = 3/1 mode without considering the plasma response. With RMPs, the toroidal velocity significantly increases in the direction of the plasma current in the q=3 resonant layer. The shapes of the radial profiles of the electron temperature are significantly different with and without RMPs. Without RMPs, the electron

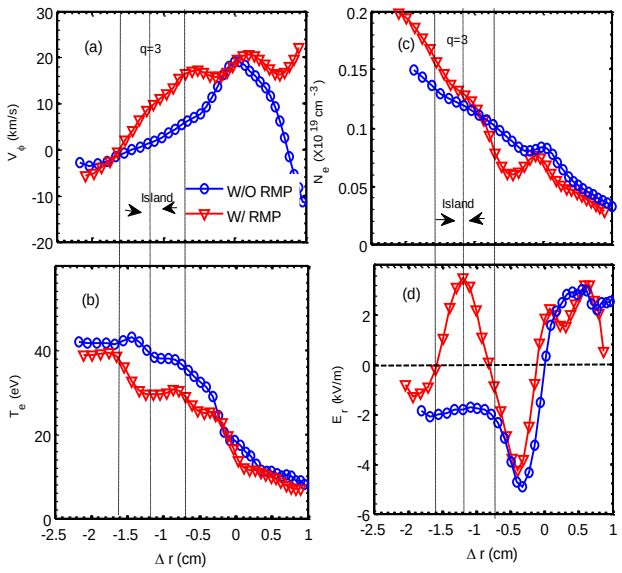

Figure 4 (color online) Radial dependences of plasma parameters with and without RMPs at q_a=3.2, (a) toroidal rotation velocity, (b) electron temperature, (c) electron density, (d) radial electric field [The vertical dashed-dot line indicated the q=3 resonant surface, B_t~1.6T, I_p~160kA, q_a=3.2, N_e~3.0x10^{19}m^{-3}].

temperature increases inward, while with RMPs, the electron temperature drops and becomes flattened around the q=3 resonant surface. The T_e flat is identified as a direct effect of RMP-induced islands in the previous observation, i.e., with magnetic islands, T_e is flattened inside the islands, while T_e becomes steeper at the island boundaries [11]. The island width is estimated as ~1.0cm from the temperature profiles. In this discharge, the electron density does not drop near the q=3 resonant surface with RMPs, as shown in figure 4 (c). The radial electric field changes from negative to positive inside the magnetic islands. This result suggests that the increase of the toroidal rotation velocity is due to the effects of RMP-induced islands.

3.3 Radial dependences of plasma parameters with 4/1 RMPs

The radial dependences of the plasma parameters with and without 4/1 RMPs at q_a=4.3 are also studied. The radial profiles of the toroidal rotation velocities at q_a=4.3 with and without RMPs are given in figure 5(a). The RMP current is ~5kA and produces a relative magnetic perturbation B_r/B_0 ~ 3 x 10^{-5} for the m/n = 4/1 mode without considering the plasma response. The line averaged density is ~2.2x$10^{19}m^{-3}$. Without RMPs, the toroidal rotation is in the counter-current direction around the q=4 resonant surface in the interval -2.5 < Δr <-0.7cm. With RMPs, the toroidal velocity sharply increases around the q=4 resonant surface in the co-current direction. This is similar to the case with 3/1 RMPs. Moreover, the toroidal rotation in the interval -2.5 < Δr < -0.7cm changes its sign from the counter-current direction to the co-current direction. The

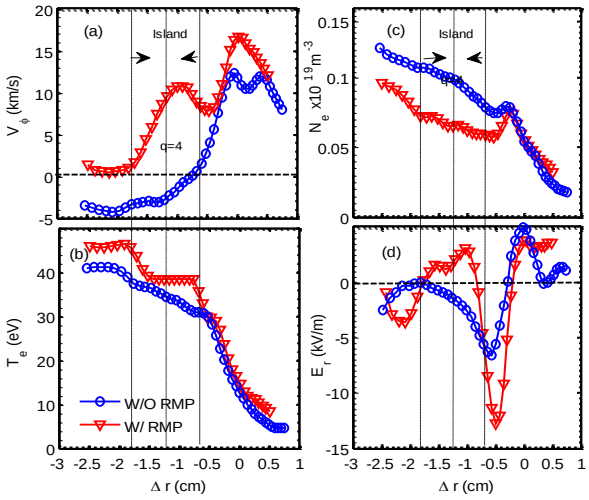

Figure 5 (color online) Radial dependences of plasma parameters with and without RMPs at q_a=4.3, (a) toroidal rotation velocity, (b) electron temperature, (c) electron density and (d) radial electric field [N_e ~ 2.2 × 10^{19} m^{-3}, I_p~150kA, B_T ~ 2.0 T].

reversal of the toroidal rotation is not observed with 3/1 RMPs. Similarly, the electron temperature is flattening inside the island and becomes steeper at its boundaries, as shown in figure 5 (b). However, T_e in the island region does not drop. This differs from the cases with 3/1 RMPs, where T_e significantly drops inside the island. Figure 5 (c) presents the radial profiles of the electron density with and without RMPs. Compared with the cases with 3/1 RMPs, the density significantly drops inside the islands. There is no significant difference for the E_r profiles in the 3/1 and 4/1 island regions. With 4/1 islands, the E_r also increases around the q=4 resonant surface, as given in figure 5 (d).

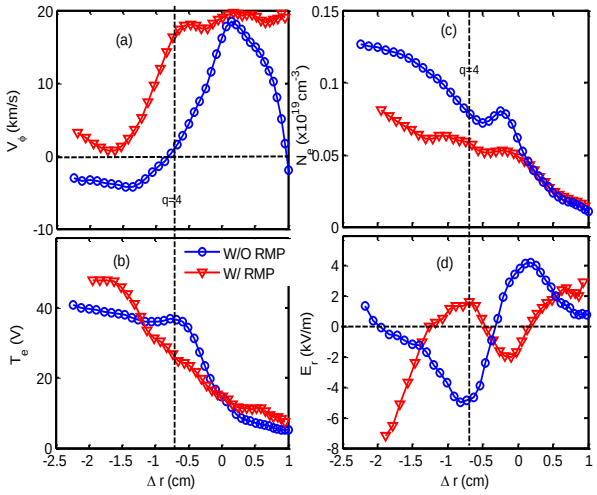

Figure 6 (color online) Radial dependences of plasma parameters with and without RMPs at q_a=4.3, (a) toroidal rotation velocity, (b) electron temperature, (c) electron density, (d) radial electric field [$N_e \sim 2.2 \times 10^{19}$ m^{-3}, $I_p \sim$ 150 kA, $B_T \sim$ 1.9T].

The radial dependences of the plasma parameters with and without 4/1 RMPs at q_a=4.1 are investigated to understand the effects of resonant layer positions on the toroidal rotations. Figures 6(a)-(d) provide the profiles of the toroidal rotation velocities, the electron temperatures, the electron densities, and the radial electric fields (E_r), respectively. The RMP current keeps at ~ 5kA and the density is ~2.2x10$^{19}m^{-3}$. With RMPs, the toroidal rotation also increases in the co-current direction near the q=4 resonant surface and are similar to the case with q_a=4.3. Compared with the cases with q_a=4.3 and 3.2, the T_e flat vanishes near q=4 resonant

surface although the T_e drops there. The steeper T_e profile also forms in the interval $-1.7 < \Delta r < -0.7$cm. The disappearance of the T_e flat might come from that the q=4 resonant layer is closer to the LCFS so that the RMP-induced islands touch the limiter, or a stochastic region forms. Around the q=4 surface, the density drops with RMPs at q_a=4.1 and is consistent with the case with q_a=4.3. With RMPs, the sign of the E_r around q=4 surface changes from negative to positive at q_a=4.1. This is similar to those observed in the cases with q_a=3.2 and 4.3. Furthermore, the E_r becomes flattened near the LCFS with RMPs at q_a=4.1, i.e., increases inside the LCFS and decreases outside the LCFS.

3. 4 Characteristics of turbulence around resonant surfaces with RMPs

The characteristics of turbulence around the resonant surfaces with RMPs are examined for q_a=4.3. The root mean square amplitude of the floating potential fluctuations in the frequency band of 30-400 kHz is provided in figure 7 (a). The turbulence intensity drops significantly, by up to 30%, inside the magnetic island, and

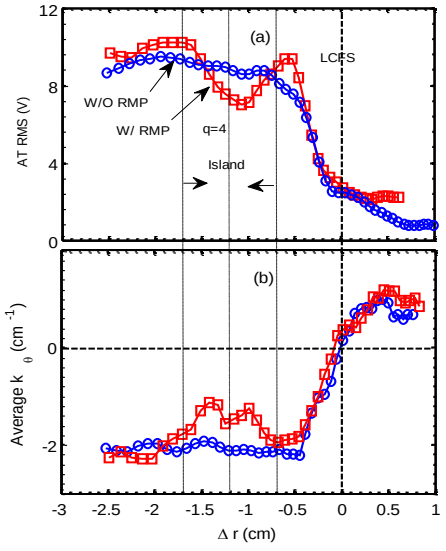

Figure. 7 (color online) Radial profiles of turbulence intensity (a) and averaged poloidal wave-vector (b) without (blue squares) and with (red circles) RMPs [The positive (negative) sign of wave-vector indicates the ion (electron) diamagnetic direction, N_e~2.2x10^{19}m^{-3}, B_t~2.0T, I_p~150kA].

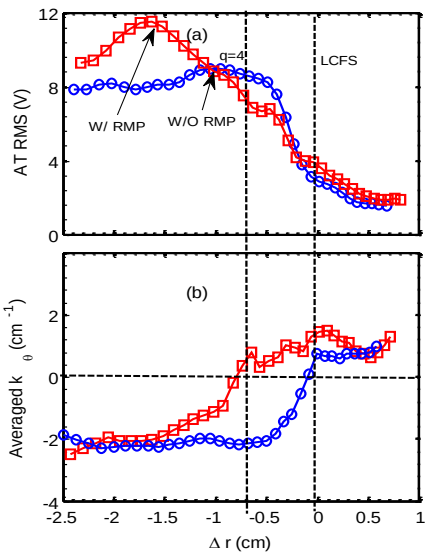

Figure. 8 (color online) Radial profiles of turbulence intensity (a) and averaged poloidal wave-vector (b) without (blue squares) and with (red circles) RMPs [The positive (negative) sign of wave-vector indicates the ion (electron) diamagnetic direction, N_e~2.2x10^{19}m^{-3}, B_t~1.9T, I_p~150kA].

increases at its boundary. The island effects on turbulence lead to the formation of the negative gradient layer of turbulence intensity in the interval -1.7< Δr < -1.2cm. The radial profiles of the weighted average of the poloidal wave number k_θ for the turbulence are also shown in figure 7 (b). The k_θ is calculated with the cross-phase analysis. The negative k_θ inside the LCFS indicates that the turbulence propagates in the electron diamagnetic drift direction. In the island regime, the k_θ increases.

The root mean square amplitudes of the floating potential fluctuations in the frequency band of 30-400 kHz with and without RMPs at q_a=4.1 are given in figure 8 (a). With RMPs, the turbulence intensity also drops near the q=4 resonant surface of Δr ~-0.7cm. The negative gradient layer of turbulence intensity is established in the interval -1.7 < Δr < -0.5cm. The poloidal wave number k_θ of the turbulence increases in the regime from Δr =-1.5 to -0.0cm, as shown in figure 8 (b). In the interval -0.7< Δr < -0.0cm, the sign of the k_θ changes from negative to positive. The positive k_θ suggests that the turbulence moves in the ion diamagnetic drift direction.

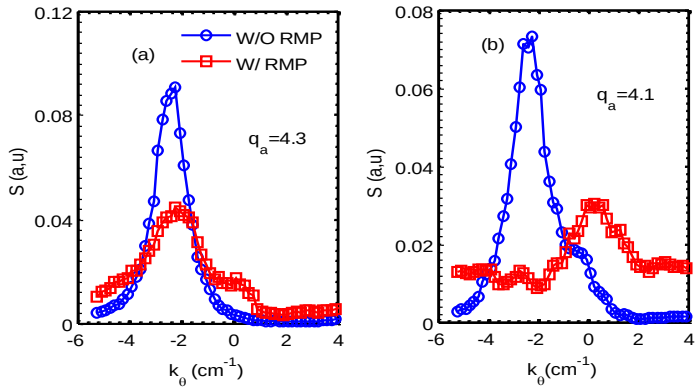

Figure. 9 (color online) Radial profiles of the $S(k_\theta)$ spectra for q_a=4.3 (a) and q_a=4.1 (b) with and without RMPs. (N_e~2.2x$10^{19}m^{-3}$, B_t~1.9-2.0T, I_p~150kA).

The poloidal wave-amplitude spectrum $S(k_\theta)$ of the turbulence is examined for the cases with and without RMPs to obtain more information for the turbulence. The $S(k_\theta)$ spectrum is estimated with two point correlation techniques [37]. Based on the wave number-frequency spectrum $S(k, f) = 1/M \sum_{i=1}^{m} I[k - k_i(f)] S_{crs,i}(f)$, the

spectral averaged wave number can be derived. Here, $I\,(a-b)$ = 1 if $a = b$, otherwise, $I\,(a-b)$ = 0, $S_{crs,i}(f)$ and M represent the cross-correlation function and the number of realizations, respectively. Figure 9 (a) presents the $S(k_\theta)$ spectra near resonant surfaces with and without RMPs at q_a=4.3. With RMPs, the $S(k_\theta)$ spectra are broadening and the power fraction of turbulence for the positive k_θ components increases. At q_a=4.1, the $S(k_\theta)$ spectra become wider and the power fraction of turbulence for the positive k_θ components more significantly increases with RMPs than those of the cases with q_a=4.3, as shown in figure 9(b). This result suggests that the characteristics of turbulence are significantly changed around resonant surface due to RMPs.

3. 5 Turbulent Reynolds stress around resonant surface with RMPs

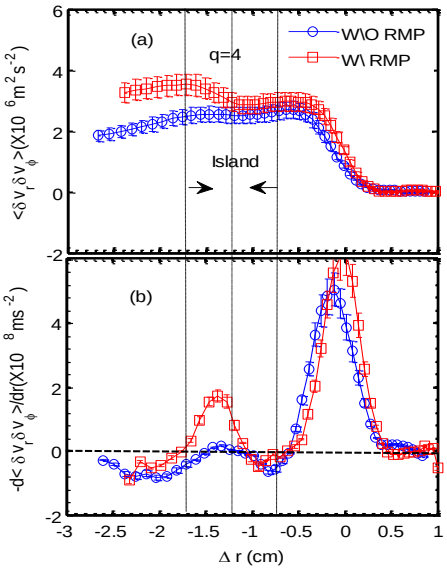

Figure. 10 (color online) Radial profiles of turbulent Reynolds stress (a) and its gradient (b) with and without RMPs at q_a=4.3.

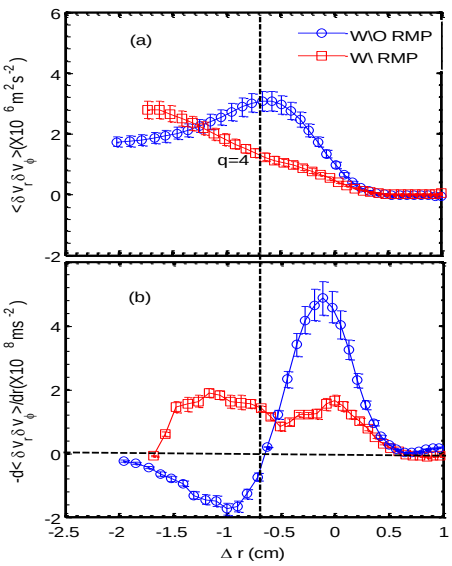

Figure. 11 (color online) Radial profiles of turbulent Reynolds stress (a) and its gradient (b) with and without RMPs at q_a=4.1.

To understand the interaction of toroidal flows with turbulence around resonant surface, turbulent Reynolds stress and its gradient are measured and presented in

figures 10 (a) and (b) with and without RMPs at q_a=4.3. The Reynolds stresses are estimated as $< \delta v_r \delta v_\phi >$, here, δv_r and δv_ϕ are the radial and toroidal turbulent velocities, computed from the high frequency components of the turbulence. < ... > is the time average over a time period of ~2 ms. The δv_r is estimated with floating potential fluctuations from tips at two poloidal positions. δv_ϕ is calculated as $C_s \delta M_{mach}$. Two steep gradient regimes of Reynolds stresses appear with RMPs. One is localized at the LCFS and another occurs near the q=4 resonant surface. The steep gradient of Reynolds stresses in the magnetic island region suggests that flows are driven there.

Figures 11 (a) and (b) provide the turbulent Reynolds stress and its gradient with and without RMPs at q_a=4.1. With RMPs, the Reynolds stress drops significantly near the q=4 surface. This differs from the cases with RMPs at q_a=4.3, where the Reynolds stress increases. The RMP effects on Reynolds stress induce the increase of the gradient of the turbulent Reynolds stress near the q=4 surface. This observation is consistent with the measurements of the toroidal flows with and without RMPs at q_a=4.1, i.e., the toroidal velocity significantly increases around the q=4 surface in the direction of the plasma current with RMPs.

3.6 Energy transfer between turbulence and toroidal flows

The energy transfer between turbulence and toroidal flows was evaluated. From the turbulent Reynolds stress and the derivative of the toroidal velocity, the flow

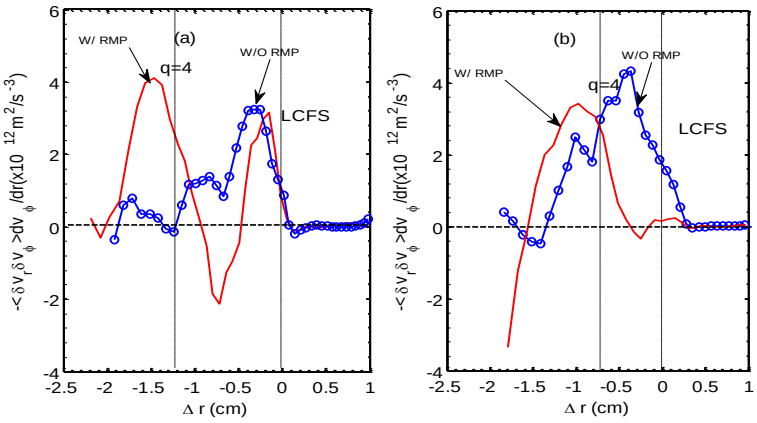

Figure. 12 (color online) Radial profiles of toroidal flow energy production with and without RMPs at (a) q_a=4.3, and (b) q_a=4.1.

energy production can be written as $P = -\langle \delta v_r \delta v_\phi \rangle \frac{dV_\phi}{dr}$ [38]. Figure 12 (a) gives the radial profiles of the energy production term P with and without RMPs at q_a=4.3. The positive (negative) p indicates the energy source (sink) for the toroidal flows. Without RMPs, the peaked energy production appears near the LCFS. With RMPs, two positive peaks for the flow energy production occur. One is localized near the LCFS, and another is near the q=4 resonant surfaces. Figure 12(b) provides the radial profiles of the energy production term P with and without RMPs at q_a=4.1. At q_a=4.1, without RMPs, the shape of the radial profiles for the flow energy production is similar to the case at q_a=4.3, i.e., the peak of the flow energy production occurs near the LCFS. However, with RMPs, the peak of the flow energy production moves to near the q=4 resonant surface. The result suggests that turbulence energy transfers into toroidal flows near the q=4 resonant surface with RMPs. In addition, the energy sink is significantly observed at q_a=4.3 with RMPs.

3.7 Conclusion and discussion

The toroidal rotation flows around the resonant surfaces with resonant magnetic perturbations are studied. These experiments were performed using a Langmuir probe array in the edge plasmas of the J-TEXT tokamak. Some common features were obtained. With RMPs, the toroidal rotation around resonant surfaces increases in the direction of the plasma current. The characteristics of the turbulence around resonant surface are significantly affected by RMPs. The turbulence intensity changes and the k_θ increases with RMPs. The power fraction of the turbulence components in the ion diamagnetic drift direction increases with RMPs. The measurements of turbulence Reynolds stresses are consistent with that the toroidal flows may be driven by turbulence. The estimations of the energy transfer suggest that turbulence energy transfers into toroidal flows.

The observation shows that the acceleration of the co-current toroidal rotation with RMPs is well correlated with the change of turbulence characteristics. The measurements of the turbulent stresses and the energy transfer between flows and turbulence with and without RMPs suggests that the momentum (energy)

redistribution takes place due to the turbulence force with RMPs, i.e., the momentum (energy) sources or sinks occur near the resonant surface. Thus, the observation has the implication of the intrinsic rotation being affected by RMPs. This result suggests that RMPs can be as a tool to change the characteristics of the edge turbulence, and thus control the intrinsic rotations in the edge tokamak plasmas.

Acknowledgments: This work is supported by the fund of State Key Laboratory of Advanced Electromagnetic Engineering and Technology in HUST (2016KF008); by National Science Foundation of China, Nos. 11175060, 11175058, 11375054, 91130031, 11320101005 and 11075046; by the National Magnetic Confinement Fusion Science Program Nos.2013GB107001, 2014GB107000 and 2013GB112008.

Reference

[1] Seanp Matt, et al., *APJ*, **754**, L26 (2012).

[2] Balbus S A and Hawley J F, *APJ*, **376**, 241(1991).

[3] Balbus S A and Hawley J F, *Rev. Mode. Phys*. **70**, 1,(1998).

[4] Aubert J and Fournier A, *Nonlin. Processes Geophys*. **18**, 657(2011).

[5] Jakubowski M W et al., *Phys. Rev. Lett*. **96**, 035004 (2006).

[6] Unterberg B et al., *Journal of Nuclear Materials*, **390-391**, 351 (2009).

[7] Schmitz O et al., *Nuclear Fusion*, **52**, 043005(2012).

[8] Schmitz O et al., *Journal of nuclear materials*, **390**, 330(2009).

[9] K.H. Finken et al., *Nucl. Fusion*, **47**, 522 (2007).

[10] Ida K et al., *Phys. Rev. Lett*. **88**, 015002 (2001).

[11] Zhao K J et al, *Nucl. Fusion*, **55**, 073022 (2015).

[12] Xu Y et al., *Phys. Rev. Lett.* **97**, 165003 (2006).

[13] Xu Y et al., *Nucl. Fusion*, **47**, 1696 (2007).

[14] Leconte M and Diamond P H, *Phys. Plasmas* **19**, 055903 (2012).

[15] Evans T E et al *Phys. Rev. Lett.* **92,** 235003 (2004).

[16] Rice J E *et al Nucl. Fusion* **39** 1175 (1999).

[17] Rice J E *et al Nucl. Fusion* **44** 379 (2004).

[18]Takechi M *et al* 2007 *Phys. Rev. Lett.* **98** 055002.

[19] Berkery J W *et al* 2010 *Phys. Rev. Lett.* **104** 035003.

[20] Diamond P H et al *Nucl. Fusion* **53,** 104019, (2013).

[21] Yan Z *et al Phys. Rev. Lett.* **104** 065002 (2010).

[22] Rice J E *et al Phys. Rev. Lett.* **106** 215001(2011).

[23] Rice J E *et al., Nucl. Fusion, **47**,1618(2007).*

[24] Y J Shi et al., *Phys. Rev. Lett, **106**,235001(2011).*

[25] Yoshida M et al., *Phys. Rev. Lett.* **100,** 105002 (2008)

[26] Wang L and Diamond P H, *Phys. Rev. Lett.* **110**, 265006 (2013).

[27] Tamain P *et al*., *Plasma Phys. Control. Fusion* **52**, 075017 (2010).

[28] J.W. Coenen, et al, *Nucl. Fusion*, **51**, 063030 (2011).

[29] Unterberg B et al., *Journal of Nuclear Materials*, **363–365**, 698(2007).

[30] Stoschus H et al., *Phys. Plasmas* **17,** 060702 (2010).

[31] Kraemer-Flecken A, et al., J. Plasma Fusion Res.Series, **8**, 44 (2009).

[32] LaHaye R J *et al., Phys. Plasmas* **1,** 373 (1994).

[33] Garofalo A M *et al Phys. Rev. Lett.* **101,** 195005 (2008).

[34] Finken K H et al., *Phys. Rev. Lett*, **94**, 015003 (2005).

[35] Zhuang G. *et al., Nucl. Fusion* **51** 094020 (2011).

[36] Rao B *et al., Fusion Eng. Des.* **89** 378 (2014).

[37] Beall J M *et al., J. Appl. Phys*. **53**, 3933 (1982).

[38] Goncalves B *et al., Phys. Rev. Lett.* **96,** 145001(2006).